

A novel structural element accounts for the constitutive activity of the orphan nuclear receptor, LRH-1

Elena P. Sablin^{1,3}, Irina N. Krylova^{2,3}, Robert J. Fletterick¹, and Holly A. Ingraham^{2*}

Department of Biochemistry and Biophysics¹ and Physiology²
University of California San Francisco
San Francisco, California 94143

³ These authors contributed equally to the work

*Corresponding Author: Email: hollyi@itsa.ucsf.edu

Running title: **Crystal Structure of the LRH-1 LBD**

SUMMARY

The orphan nuclear receptors, SF-1 and LRH-1 are constitutively active, but it remains uncertain whether their activation is dependent on hormone. Here we report the crystal structure of the LRH-1 ligand-binding domain to 2.4Å resolution and show the receptor in an active conformation with a large, but empty hydrophobic pocket. This active conformation was achieved without the stabilizing influences of ligand, coactivator peptide or receptor partners. Adding bulky side chains into the pocket resulted in full or greater LRH-1 activity suggesting that while this “ligand-binding pocket” could easily accommodate potential agonists or antagonists, such ligands are dispensable for basal activity. Constitutive activation of LRH-1 appears to be mediated by a novel structural element consisting of an extended rigid helix 2, which provides an additional fourth layer to the typical three-layered fold present in other LBD structures. We propose that this subfamily-specific helix positioned outside of the LBD pocket mediates receptor stabilization similar to ligand binding inside the pocket.

INTRODUCTION

Liver related homologue 1 (LRH-1, NR5A2) and steroidogenic factor 1 (SF-1, NR5A1) are orphan nuclear receptors that define subfamily V of this large gene family. Both SF-1 and LRH-1 share conserved signature motifs characteristic of nuclear receptors that include a DNA binding domain (DBD), a putative ligand binding domain (LBD), and a hinge region separating the DBD and LBD. SF-1 and LRH-1 bind DNA with high affinity as monomers, making them distinct from other homodimeric or heterodimeric receptors. SF-1 is required for proper male sexual development (Roberts et al., 1999) and development of endocrine and neuroendocrine tissues (Ingraham et al., 1994; Luo et al., 1994; Parker et al., 2002; Sadovsky et al., 1995; Tran et

al., 2003). Although the precise developmental roles for LRH-1 have yet to be defined, both SF-1 and LRH-1 coordinately regulate genes involved in steroid and bile acid/cholesterol homeostasis, respectively (Goodwin et al., 2000; Hammer and Ingraham, 1999; Lu et al., 2000). Expression of SF-1 is high in both the steroid producing adrenal glands and gonads (Parker et al., 2002), whereas LRH-1 is found in the liver and intestine, where it regulates genes encoding key enzymes in bile acid synthesis, such as *CYP7A* and *CYP8B1* (del Castillo-Olivares and Gil, 2000; Nitta et al., 1999), as well as genes involved in cholesterol transport (Luo et al., 2001; Schoonjans et al., 2002). In instances where SF-1 and LRH-1 are coexpressed, deciphering the specificity of target genes can be difficult because both receptors bind similar sites with equal affinities. Indeed, while SF-1 was assumed to regulate *CYP19* encoding the aromatase enzyme that converts androgen to estrogen (Fitzpatrick and Richards, 1993), expression patterns of these two receptors during follicular maturation showed LRH-1, and not SF-1, as the major regulator of ovarian aromatase (Hinshelwood et al., 2003; Liu et al., 2003).

The existence of an SF-1 or LRH-1 agonist has not been demonstrated, consistent with the fact that both receptors activate reporter constructs in the apparent absence of ligand. While oxysterols have been proposed to activate SF-1, their role as bona fide SF-1 ligands remains controversial because they fail to activate SF-1 further in several cellular contexts, and fail to confer conformational changes expected upon ligand binding (Desclozeaux et al., 2002; Lala et al., 1997; Mellon and Bair, 1998). Whether regulation of LRH-1 and SF-1 is ligand-independent or is instead achieved by low-affinity, non-specific ubiquitous ligands, as suggested by some LBD structures (Dhe-Paganon et al., 2002; Stehlin et al., 2001; Wisely et al., 2002), remains an unresolved issue.

For ligand-dependent receptors, hormone binding induces conformational changes that include a critical repositioning of the C-terminal helix H12 within the activation function (AF2) region (Nolte et al., 1998). Similar to other receptors, LRH-1 and SF-1 possess an intact and functional AF2 domain (Galarneau et al., 1996; Ito et al., 1997). Further analyses of SF-1 mapped a second activation region to the predicted helix H1, which is referred to as AFH1 (Crawford et al., 1997; Desclozeaux et al., 2002). The N-terminal LBD region in LRH-1 and SF-1, including helices H1-H3, is highly conserved and subfamily V-specific, with virtually no sequence similarity shared with other receptor subfamilies (Giguere, 1999). For ligand-dependent receptors, this subfamily specific N-terminal region associates with the remaining LBD in a receptor-specific and ligand-dependent manner (Pissios et al., 2000). This is not the case with SF-1, where robust assembly is observed independent of exogenous ligand (Desclozeaux et al., 2002). For subfamily V receptors, posttranslational modification of the hinge region just N-terminal to helix 1 provides an additional site for receptor regulation. Indeed, MAPK phosphorylation at serine S203 in SF-1 (the LBD begins at Pro224) enhanced receptor activity and cofactor recruitment (Desclozeaux et al., 2002; Hammer et al., 1999). Although two potential MAPK phosphorylation sites in the hinge region of LRH-1 have yet to be investigated, stimulation of the MAPK pathway increases LRH-1 activation of the aromatase promoter, implying that LRH-1 activity is also modulated by phosphorylation (I.N.K., unpublished results).

Structural analysis of ligand-dependent receptors have established that ligand-controlled positioning of helix H12 in the AF2 region influences recruitment of coregulators, including coactivators and corepressors (Darimont et al., 1998; Glass and Rosenfeld, 2000; Nolte et al.,

1998; Shiau et al., 1998). Three-dimensional modeling of the SF-1 LBD based on the structure of the closest homologue RXR , suggested that both SF-1 and LRH-1 LBDs would adopt an active conformation in the absence of ligand (Desclozeaux et al., 2002). In vitro data suggests that while coregulator binding by SF-1 and LRH-1 appears to be ligand-independent, binding affinities are markedly lower compared with ligand-dependent receptors ((Hammer et al., 1999), and H.A.I. unpublished data), raising the possibility that these coregulators play a less crucial role in SF-1 and LRH-1 function. Tissue-specific repressors for both LRH-1 and SF-1 have been proposed, and include the orphan receptors Dax-1 and SHP. The first receptor, Dax-1 is capable of antagonizing both SF-1 and LRH-1-mediated transcription, in vitro (Ito et al., 1997; Nachtigal et al., 1998; Suzuki et al., 2003), but is linked more closely with SF-1 by the shared clinical adrenal phenotypes exhibited by *SF-1* and *DAX1* human mutants (Achermann et al., 2001). The second receptor, SHP or small heterodimeric partner, also represses both SF-1 and LRH-1 (Lee and Moore, 2002; Suzuki et al., 2003). Targeted deletion of *Dax-1* and *SHP* genes in mice supports partially the proposal that these two repressors modulate SF-1 or LRH-1 activity, to indirectly influence steroid and bile acid homeostasis, respectively (Goodwin et al., 2000; Kerr et al., 2002; Lu et al., 2000; Wang et al., 2002; Wang et al., 2001).

Here, we have undertaken a crystallographic analysis of LRH-1 to determine how this nuclear receptor achieves a constitutively active form and whether ligand is required for its activity. We find that unlike other members of the family, a stable active monomeric LRH-1 LBD can exist in the absence of ligand, coactivator peptide, or a homo- or heterodimeric receptor partner.

RESULTS

Crystal structure of LRH-1 LBD

Crystals of LRH-1 ligand binding domain were obtained as described in Methods and Materials. The structure of LRH-1 LBD was determined by the molecular replacement method using an atomic model of the hormone-bound RXR LBD (Egea et al., 2000). The current LRH-1 model is refined to 2.4 Å resolution with R/R_{free} values of 21.3/23.1 and consists of residues A318-R559 (Table 1). The LBD of LRH-1 shares a common fold found in other receptors, but contains an additional fourth layer, instead of the typical three-layered sandwich of eleven helices and two short α -strands (orange, purple and pink layers, Fig. 1A, B). Superposition of LRH-1 with its closest structural relative hormone bound RXR revealed a conformation that resembles an active, agonist-bound state of ligand-dependent receptors where the C-terminal helix H12 is packed tightly against the H3-H4-H5-H11 region of the LBD (Fig. 1C). Furthermore, superposition of C α atoms from helices H3, H4, H5, H11 and H12 that define the transcriptionally active state of AF2 region shows a r.m.s.d. value of 1.0 Å, confirming the active conformation of the LRH-1 LBD.

The LRH-1 structure exhibits three distinct features not present in other LBD structures. The first and most striking feature of LRH-1 is the rigid and relatively long helix H2, which is packed tightly against helix H3 and forms an additional, fourth outer layer in the receptor's structure (Fig. 1A, B, in red). In most nuclear receptors, as shown here for RXR (Fig. 1C), the region connecting helices H1 and H3 forms a flexible loop that is often partially disordered. The spatial configuration of the extended H2 in LRH-1 contrasts the short helical fragments termed H2 (and H2') that have been observed in other nuclear receptor structures (PPAR α , PPAR β , PPAR γ ,

ROR , ROR , VDR), where only a loose contact is made with the rest of the receptor's body (Kallen et al., 2002; Nolte et al., 1998; Stehlin et al., 2001; Xu et al., 1999; Xu et al., 2002). The other two related characteristic features of the LRH-1 LBD are the positions of the preceding helix H1 and the N-terminal linker. In LRH-1, helix H1 is translated by one helical turn towards H9 and thus differs from other receptors (Fig. 1C). As a consequence of this shift, packing interactions of helix H1 are altered so that the N-terminal proline (P321) is configured on the opposite face of helix H1 and is likely to influence the direction of the N-terminal linker of LRH-1, which runs along helix H9. We note that all three unique LRH-1 structural features are strategically positioned on the outside surface of the LRH-1 LBD (Fig. 1A, B).

LRH-1 contains a large, well-formed but empty ligand binding pocket

Consistent with the fact that the LRH-1 LBD was expressed in *E.coli* and crystallized without a known natural or synthetic ligand, the structure revealed no ordered ligand in the ligand binding cavity of the receptor (Fig. 2A). Nevertheless, the LRH-1 hormone pocket is large ($\sim 820 \text{ \AA}^3$), well defined and fully enveloped or "closed" by 28 amino acid residues lining its walls (Fig. 2A, B). The ligand-binding cavity of LRH-1 is mostly hydrophobic, but contains one hydrophilic region comprised of three charged residues D408, H409 and a R412, from helix H5. The highly conserved R412 forms an ionic pair or salt bridge with D408. Examination of the pocket by superimposition with other liganded structures suggests that the overall shape and size of LRH-1 pocket easily accommodates ligands such as 9-cis retinoic acid (Fig 2B) or a cholesterol-like ligand (Kallen et al., 2002). Thus, the overall architecture of the LRH-1 pocket is similar to other ligand-dependent receptors

The existence of a well-formed cavity within the LRH-1 LBD might imply that a specific ligand is required for full receptor activity *in vivo*, as demonstrated for other orphan nuclear receptors (Greschik et al., 2002; Watkins et al., 2001). To test whether LRH-1 activity might be ligand-dependent, single amino acid mutations were created to fill the ligand-binding pocket of LRH-1. Specifically, small side chains facing inside the pocket (A368 and A532 from helices H3 and H11, respectively) were substituted with bulkier residues that would interfere with binding of a putative ligand. The predicted dramatic effect on the size and shape of the LRH-1 ligand-binding pocket is illustrated for one such mutant, A368W (Fig. 2D). Unexpectedly, we found that all four mutants including A368W, A368M, A532W and A532M exhibited activity comparable to that of wild type LRH-1 when tested in HepG2 liver cells, which express endogenous active LRH-1 (Galarneau et al., 1996) (Fig 2E). While designed variants rarely improve on nature, we found that H11 pocket mutants (A532W, A532M) exhibited consistently higher activity than wild type or H3 mutant receptors (Fig 2E). Similar results were obtained using a mammalian two-hybrid system (data not shown). The increased activity of H11 mutants might reflect further stabilization of LRH-1 structure via additional hydrophobic interactions contributed by altered side chains of helix H11, which is normally more rigid than H3. Activities of all four pocket-mutants were repressed after adding the orphan nuclear receptor SHP, however this repression was diminished in H11 mutants (Fig 2E). Collectively, these data imply that LRH-1 activity is preserved even after disrupting the size and shape of its ligand-binding pocket.

Architecture of the coactivator-binding cleft of LRH-1

To determine if LRH-1 is capable of promoting coactivator binding, we evaluated the fit of the Grip NR-box 2 peptide in the LRH-1 coactivator binding cleft by computational modeling. As

shown in Fig 3A, LRH-1 LBD structure is competent to bind a LXXLL coactivator peptide (blue helix). However, we noted that helix H12 is shifted slightly towards the coactivator-binding groove in LRH-1, with an r.m.s.d. value of 1.5 Å when compared with H12 of RXR complexed with a coactivator peptide (Fig. 3A). More importantly, optimal peptide docking to LRH-1 is achieved only after adjustment of side chains in LRH-1-specific residues, which include R380 (H3), Q398 and M394 (H4) and N549 (H12) (Fig. 3B). R380 is usually a conserved lysine in other receptors, and is part of the so-called “electrostatic clamp” stabilizing receptor-coactivator complex (Darimont et al., 1998). The shorter and uncharged side chain of Q398, which is usually an arginine or lysine in other receptors, might not stabilize the position of the C-terminal of H12. The other two residues M394 and N549, are not the usual small hydrophobic or polar residues (A/S/T/V/P) present in most receptors, but instead possess bulkier side chains that could potentially interfere with coactivator docking. To investigate whether an “optimized” LRH-1 coactivator cleft might enhance coregulator function, two of four LRH-1-specific residues were replaced to match their counterparts in RXR (M394V and N549T, referred to as the mCleft mutant). We reasoned that altering the bulkier M394 and N549 might yield more dramatic results because flexible side chains of R380 and Q398 could adjust their conformations to retain important interactions. Activation of the mCleft LRH-1 mutants by nuclear receptor coregulators was significantly elevated compared to wild type receptor (Fig. 3C). Collectively, these data suggest that while coregulator recruitment by LHR-1 is ligand-independent, binding of known nuclear receptor coactivators via the LRH-1 cleft is not optimized.

Helix 2 contributes to binding of coregulators

Given that the LRH-1 helix H2 indirectly supports the position of helix H12, we examined the possible functions of this novel element on LRH-1 activity. To do this, three polar amino acid residues on the solvent exposed side of H2 (Q336, Q346, and Q347) were substituted with either alanines or histidines (Fig 4A). This triple LRH-1 mutant (Q336A/Q346A/Q347H, referred to as mQ3) showed diminished activity in HepG2 cells when cotransfected with either the co-activator AIB1 (Fig 4B) or the corepressor SHP (Fig. 4C). These results were supported further by mammalian two-hybrid data showing that interactions of the mQ3 LRH-1 mutant receptor with VP16mSHP1 and GRIP1 were lessened (Fig 4D and data not shown). Assuming that there is no change in stability of helix H2 in the mQ3 mutant, these data suggest that residues on the exposed surface of H2 might provide a new binding interface for regulatory proteins.

The monomeric nature of LRH-1/SF-1

In contrast to nuclear receptors that form homo- or heterodimers, both LRH-1 and SF-1 bind DNA with high affinity as monomers (Galarneau et al., 1996; Nachtigal et al., 1998). Consistent with these data, only monomers were found in the LRH-1 crystals. Furthermore, analytical ultracentrifugation analyses showed that the LRH-1 LBD forms a homogeneous population of monomers in solution (Fig 5A). Because the dimerization interface is topologically conserved in all LBD homo- and heterodimer structures (Gampe et al., 2000; Moraitis and Giguere, 1999; Ribeiro et al., 2001), an LRH-1 homodimer was modeled by superposing the LRH-1 with LBDs of an active RXR homodimer. Consistent with our biochemical data, this LRH-1 homodimer model generated a number of steric clashes and repulsive interactions at the virtual dimerization interface. The most obvious pair of repulsive contacts is generated between two glutamic acid

residues, E494 and E513 from helices H9 and H10, respectively (Fig 5B). Remarkably, E513 at the beginning of H10 is a family-specific substitution for the small non-charged residue commonly found in all dimeric receptors (G in RXR , Fig 5C). Assuming that E494 and E513 are charged, these repulsive contacts alone would be sufficient to destabilize a canonical homodimer and could explain the preferred monomeric state of LRH-1. Furthermore, destabilization of any canonical heterodimer is expected because of similar repulsive interactions between the highly conserved E494 in H9, and E513 in H10 of LRH-1 (Fig 5C). Given the high sequence similarity shared between LRH-1 and SF-1 in this region (Fig. 5C), the LRH-1 structure accounts for the distinctive monomeric binding sites present in both LRH-1 and SF-1 target promoters.

DISCUSSION

Our study shows the LRH-1 LBD in an active conformation with a large empty hydrophobic cavity and an additional fourth outermost layer, not present in other nuclear receptors. For ligand-dependent receptors, hormone binding induces conformational changes that include a critical repositioning of the C-terminal helix H12 to allow for coregulator recruitment. In the LRH-1 structure, proper positioning of helix H12 is achieved in the absence of a ligand or coactivator peptide, suggesting a ligand-independent mode of activation. These features place LRH-1, and by analogy SF-1, in a unique category and suggest that stability of the active LRH-1 LBD conformation is controlled by different mechanisms. We propose that the constitutive activation of LRH-1 and SF-1 is mediated by a novel and family-specific structural element consisting of an extended rigid helix 2. Packing interactions of this helix with the core structural

elements would provide sufficient stabilization energy to favor the activated receptor's state in the absence of hormone or coactivator.

Stability of the LRH-1 active conformation in the absence of a bound ligand

For many orphan nuclear receptors, the existence of ligands remains a controversial question. Structural analyses of many so-called “orphan” receptors revealed the presence of fortuitous ligands that copurified with the LBDs (Billas et al., 2001; Dhe-Paganon et al., 2002; Stehlin et al., 2001; Wisely et al., 2002). These low affinity pseudo-ligands, together with coactivator peptides, are proposed to stabilize the LBD and prevent it from collapsing during crystallization experiments (Stehlin et al., 2001). In the case of LRH-1, neither a pseudo-ligand, a dimerization partner, nor a coactivator peptide were required to achieve a stable LBD conformation. Thus, although the structure of LRH-1 represents the sixth reported LBD without a bound ligand (the other five include RXR , PXR, ERR3, PPAR , and PPAR (Bourguet et al., 1995; Greschik et al., 2002; Nolte et al., 1998; Watkins et al., 2001; Xu et al., 1999)), this is the first ligandless LBD structure obtained without any outside (bound coactivator/corepressor peptides, dimerization receptor partners) or inside (ligands) stabilization factors. Furthermore, in four known apo-LBD structures (PXR, ERR3, PPAR , and PPAR), the ligand-binding pocket is solvent accessible or “open” and therefore filled with solvent molecules that could provide additional stabilization of the pocket. The only hormone-binding pocket that is fully enveloped or “closed”, as shown here for LRH-1, is that of the collapsed, inactive apo-structure of RXR . Taken together we suggest that the LRH-1 structure is the first to exhibit an active conformation with a fully enveloped, but unoccupied hormone-binding pocket.

Structural model for LRH-1 activation

We propose that in the absence of cognate hormone, the active conformation of LRH-1 LBD is maintained because of the stabilizing effect of the subfamily-specific helix H2 that is packed tightly against the body of the receptor. Based on existing LBD structures, seven structural elements define the hormone binding pocket of the LBD (Steinmetz et al., 2001)(Fig 6A). We find that H2 interacts directly with four structural elements forming the walls of the pocket, including helices H3, H5, the hairpin loop, and the loop connecting H11 and H12 (Fig 6B). Helix H2 helps to define the position of H3 through its extensive packing interactions with H3 that account for an unexpectedly large buried surface ($\sim 1200 \text{ \AA}^2$), (Fig 6C). In turn, helix H3 interacts directly with the remaining three structural elements (H7, H11 and H12) of the ligand binding pocket. Thus, we postulate that helix H2 controls both the architecture of the pocket and conformational state of the LBD by either directly or indirectly interacting with all seven elements that define the conformational state of the LBD. As mentioned above, sequence alignment shows that the interacting faces of helices H2 and H3 are specific to nuclear receptor subfamily V, and have likely co-evolved to form the observed paired hydrophobic and complimentary electrostatic interactions (Fig 6C).

Helix 2 defines a unique fourth, outermost layer for LRH-1 and can be viewed as an integral “agonist” that functions outside rather than inside the ligand binding pocket. Indeed, cognate ligands and helix H2 exert similar conformational effects on the LBD of the receptor. Like receptor-specific ligands, helix H2 has a defined architecture and a subfamily-specific primary sequence that has co-evolved with the interacting surface on the body of LRH-1. Analogous to specific contacts made by the ligand, H2 interacts directly with the critical structural elements

that define the conformational state of the receptor. Thus, like some hormones that do not directly contact critical helix H12, helix H2 may still provide sufficient stabilization energy to favor an activated state of ligandless receptor. Although helix H2 is unique for LRH-1 and SF-1, other studies suggest that connecting region between helices H1 and H3 may adopt a functionally relevant, receptor family-specific conformation. Recent studies showed that the overall stability of the thyroid receptor LBD depend on the intact structure of this connecting region (Huber et al., 2003). Remarkably, the H1-H3 connecting region in the ERR3 apo-structure (Greschik et al., 2002) reveals striking similarity with helix H2 of LRH-1, as evidenced by the rigid conformation that follows the path of helix H2 in LRH-1 (Fig. 6D). We speculate that this rigid H1-H3 region in ERR3 fulfills a similar stabilizing role as helix H2 does in LRH-1, and thus, may contribute to ligand-independent activation of ERR3.

To date only one human mutation has been identified in the LBD of subfamily V receptors (Biason-Lauber and Schoenle, 2000). This reported single R255L heterozygous SF-1 mutation leads to adrenal disease with apparently normal ovarian function. This adrenal-specific phenotype is consistent with the importance of SF-1 gene dosage during adrenal organogenesis (Bland et al., 2000) and suggests a partial loss of function in this particular SF-1 mutation. Remarkably, in LRH-1, this subfamily-conserved arginine (R352) is positioned at the C-terminus of helix H2 and is needed to stabilize helix H12. Because the side chain of R352 stabilizes the conformation of the H2-H3 loop by forming hydrogen bonds with its backbone, and given that H2-H3 loop positions helix H12 by supporting the H11-H12 connection, a destabilized H12 most likely accounts for the partial loss-of-function observed in this SF-1 mutant female patient.

Regulation of LRH-1 activity

While the unique helix H2 in LRH-1 LBD explains how constitutively active receptors might maintain an active conformation in the absence of ligand, a structural puzzle emerges - do ligands exist for the LRH-1 empty pocket? The existence of a well-formed and large pocket ($\sim 830 \text{ \AA}^3$) that is not filled with side chains opens the possibility that natural agonists or antagonists exist for LRH-1. Furthermore, the LRH-1 pocket retains an asymmetrical distribution of electrostatic charge commonly observed in ligand-dependent receptors. These features contrast those observed for constitutively active ERR3, whose pocket is made small ($\sim 220 \text{ \AA}^3$) by bulky side chains (Greschik et al., 2002). Because both SF-1 and LRH-1 function in the adult to affect either steroid or bile acid homeostasis, one might easily envision that potential ligands act in a classic feed-forward (agonists) or feed-back (antagonists) manner. Currently, little evidence exists for such ligands. On the other hand, it is tempting to speculate that these potential ligands are used selectively during the diverse embryonic and adult functions of SF-1 and LRH-1. Whether the “outside” stabilizing influences of helix H2 on the LBD represent an earlier or later evolutionary event than ligand binding is unclear. In this regard, others have placed SF-1 and LRH-1 as some of the oldest members of this gene superfamily (De Mendonca et al., 2002; Escriva et al., 2000) suggesting that the LRH1 LBD may be prototypic of an unspecialized nuclear receptor fold.

A second puzzle revealed by our study is the finding that the LRH-1 coactivator-binding cleft is not fully optimized for common coregulators. This could suggest that modulation by coregulators is less critical for this receptor’s function. On the other hand, these data could suggest the existence of unidentified subfamily V-specific coregulators. Because our analysis

was limited to the LBD region of LRH-1, additional domain or modifications within the flexible hinge region (i.e., phosphorylation) might be required for optimal coregulator recruitment by both LRH-1 and SF-1. Indeed, both GST-pulldown assays and direct peptide binding studies show that the LBDs of LRH-1 and SF-1 exhibit weak binding to common coactivators with little discrimination observed between coactivators versus corepressors ((Hammer et al., 1999), and I.N.K, J. Moore, K. Guy and H.A.I, unpublished results). Future structural analyses of receptor complexes and posttranslationally modified receptors, as well as the identification of natural or pharmacological ligands, should provide additional insights into LRH-1 and SF-1 biology.

METHODS AND MATERIALS

Plasmids and Cell Transfections

Pf1 plasmid (mLRH1 full length in pCI vector, Promega) was a gift from Dr Luc Belanger, University of Laval, Quebec) (Galarneau et al., 1996). A DNA fragment encoding mouse LRH-1 LBD residues 313-560 was obtained by PCR with Pfu1, using Pf1 plasmid as a template, and cloned for expression into pBH4 plasmid carrying His-6 tag and a cleavage site for TEV protease (gift from Dr. W. Lim, UCSF). All point mutation constructs used in the transient transfection assays were created using QuikChange® XL Site-Directed Mutagenesis Kit (Stratagene) and original Pf1 plasmid as a template. LRH1 activity was measured using the AroLuc reporter, as previously described (Clyne et al., 2002), which contains 534 bp of the rat aromatase promoter in pGL2 (Promega). To create the Gal4/mLRH1 fusion construct for mammalian two hybrid assay, Pf1 PCR fragment corresponding to residues 217-560 of mLRH1 was cloned into PM1 vector (Clontech) and this construct (Gal4 mLRH DBD) served as a template to create all LRH-1 point mutants. VP16mSHP1 and CDM8mSHP1 constructs were a gift from D. Moore (Baylor College

of Medicine). The reporter used in the mammalian two hybrid assay was pGAL-RE-TK as described previously (Desclozeaux et al., 2002). All LRH-1 mutants constructs were verified by DNA sequencing.

HepG2 human hepatoma cells were grown in DMEM media supplemented by 10% fetal calf serum and were transiently transfected using FuGENE 6 (Roche), according to the manufacturer's protocol. Luciferase expression was assessed using Enhanced Luciferase Assay Kit (BD PharMingen) and Monolight 2010 (Analytical Luminescence laboratory). Luciferase activities were corrected for transfection efficiency by normalizing to β -galactosidase activity. Three independent experiments were carried out for each experiment.

Protein Preparation

Protein expression of mouse LRH-1 LBD was induced in BL21(DE3) E.coli (Novagen) with 0.2 mM IPTG followed by growth at 18°C for 6 hours. His-tagged LRH-1 LBD protein was purified on a TALON (Clontech) column and eluted in 45mM of imidazole. After removal of the His-tag with recombinant TEV protease, protein was further purified on a TSKgel Phenyl-5PW column (TOSOHAAS) equilibrated with 0.6 M ammonium sulfate, 1mM EDTA and 10 mM DTT and eluted with a 0.6M to 0 of ammonium sulfate gradient, followed by chromatography on a MonoQ column (Pharmacia) equilibrated in 20 mM ammonium acetate pH 7.4, 2 mM CHAPS, 1mM EDTA, 1 mM DTT. Protein was concentrated in 100 mM of ammonium acetate, 10 mM TCEP, 1 mM EDTA and 2 mM CHAPS. The protein purity, stability and homogeneity were assessed using SDS and native PAGE, mass spectrometry (Voyager-DETM, PerSeptive

Biosystems), gel filtration (16/60 Superdex 75, Pharmacia), Dynamic Light Scattering (protein Solutions, DynaPro-MS800).

Crystallization, Data collection, model building and refinement

Vapor diffusion method was used to obtain crystals of LRH-1 LBD in which 1 μ l of protein solution (6 mg/ml) was mixed with 1 μ l of reservoir buffer containing 15% glycerol, 21% PEG 4K, 100 mM TRIS pH 8.8, 5% isopropanol and equilibrated against this buffer for 5-7 days at 15°C. Crystals were cryo-protected using the mother liquor and then flash-frozen in liquid nitrogen prior to data collection. X-ray diffraction data were measured at -180°C and collected to 2.4 Å at Advanced Light Source (Lawrence Berkeley National Laboratory) beamline 8.3.1 (= 1.1 Å) using a single crystal. Data were integrated using DENZO and scaled with SCALEPACK. The crystal was of the monoclinic space group $P2_1$ with two ligand binding domains of LRH-1 in the asymmetric unit and cell dimensions of $a=34.8$ Å, $b=127.5$ Å, $c=53.2$ Å, and $\beta=91.7^\circ$. The LRH-1 LBD structure was determined by the molecular replacement method (package CNS) using atomic coordinates for residues 266-438 (helices 3-11) of the ligand-bound RXR (Protein Data Bank ID 1FBY). Electron-density maps based on coefficients $2F_o-F_c$ were calculated from the phases of the initial model. Subsequent rounds of model building and refinement were performed using programs QUANTA (Molecular Simulations Inc) and CNS, respectively. At the later stages of the refinement, the entire structure was checked using simulated annealing composite omit maps. The current structure is refined to R/R_{free} values of 21.3/23.1 (50.0-2.4 Å). Both LRH-1 ligand binding domains present in the crystal asymmetric unit are virtually identical and include residues A318-R559. The first five N-terminal (Q313-P317) and the last C-terminal (A560) residues are disordered in both LBD

domains and not included in the current model. One hundred water molecules are in the asymmetric unit of the current model.

Analytical Ultracentrifugation.

Analytical ultracentrifugation was performed on a Beckman Optima XL-I analytical ultracentrifuge, with detection at 277 nm. LRH-1 LBD protein (8, 4, and 2 μ M) was equilibrated at 10 °C at three speeds: 8,500, 12,000, and 17,000 rotations per minute in an AnT-50 analytical rotor. The nonlinear least-squares method of the program Nonlin (3) was used to fit multiple data sets to single or multiple species models as previously described (Maluf and Lohman, 2003).

References

- Achermann, J. C., Meeks, J. J., and Jameson, J. L. (2001). Phenotypic spectrum of mutations in DAX-1 and SF-1. *Mol Cell Endocrinol* 185, 17-25.
- Biason-Lauber, A., and Schoenle, E. J. (2000). Apparently normal ovarian differentiation in a prepubertal girl with transcriptionally inactive steroidogenic factor 1 (NR5A1/SF-1) and adrenocortical insufficiency. *Am J Hum Genet* 67, 1563-1568.
- Billas, I. M., Moulinier, L., Rochel, N., and Moras, D. (2001). Crystal structure of the ligand-binding domain of the ultraspiracle protein USP, the ortholog of retinoid X receptors in insects. *J Biol Chem* 276, 7465-7474.
- Bland, M. L., Jamieson, C. A., Akana, S. F., Bornstein, S. R., Eisenhofer, G., Dallman, M. F., and Ingraham, H. A. (2000). Haploinsufficiency of steroidogenic factor-1 in mice disrupts adrenal development leading to an impaired stress response. *Proc Natl Acad Sci U S A* 97, 14488-14493.
- Bourguet, W., Ruff, M., Chambon, P., Gronemeyer, H., and Moras, D. (1995). Crystal structure of the ligand-binding domain of the human nuclear receptor RXR-alpha. *Nature* 375, 377-382.

- Clyne, C. D., Speed, C. J., Zhou, J., and Simpson, E. R. (2002). Liver receptor homologue-1 (LRH-1) regulates expression of aromatase in preadipocytes. *J Biol Chem* 277, 20591-20597.
- Crawford, P. A., Polish, J. A., Ganpule, G., and Sadovsky, Y. (1997). The activation function-2 hexamer of steroidogenic factor-1 is required, but not sufficient for potentiation by SRC-1. *Molecular Endocrinology* 11, 1626-1635.
- Darimont, B. D., Wagner, R. L., Apriletti, J. W., Stallcup, M. R., Kushner, P. J., Baxter, J. D., Fletterick, R. J., and Yamamoto, K. R. (1998). Structure and specificity of nuclear receptor-coactivator interactions. *Genes & Dev* 12, 3343-3356.
- De Mendonca, R. L., Bouton, D., Bertin, B., Escriva, H., Noel, C., Vanacker, J. M., Cornette, J., Laudet, V., and Pierce, R. J. (2002). A functionally conserved member of the FTZ-F1 nuclear receptor family from *Schistosoma mansoni*. *Eur J Biochem* 269, 5700-5711.
- del Castillo-Olivares, A., and Gil, G. (2000). Alpha 1-fetoprotein transcription factor is required for the expression of sterol 12alpha -hydroxylase, the specific enzyme for cholic acid synthesis. Potential role in the bile acid-mediated regulation of gene transcription. *J Biol Chem* 275, 17793-17799.
- Desclozeaux, M., Krylova, I. N., Horn, F., Fletterick, R. J., and Ingraham, H. A. (2002). Phosphorylation and intramolecular stabilization of the ligand binding domain in the nuclear receptor steroidogenic factor 1. *Mol Cell Biol* 22, 7193-7203.
- Dhe-Paganon, S., Duda, K., Iwamoto, M., Chi, Y. I., and Shoelson, S. E. (2002). Crystal structure of the HNF4 alpha ligand binding domain in complex with endogenous fatty acid ligand. *J Biol Chem* 277, 37973-37976.
- Egea, P. F., Mitschler, A., Rochel, N., Ruff, M., Chambon, P., and Moras, D. (2000). Crystal structure of the human RXRalpha ligand-binding domain bound to its natural ligand: 9-cis retinoic acid. *EMBO J* 19, 2592-2601.
- Escriva, H., Delaunay, F., and Laudet, V. (2000). Ligand binding and nuclear receptor evolution. *Bioessays* 22, 717-727.
- Fitzpatrick, S. L., and Richards, J. S. (1993). *Cis*-Acting elements of the rat aromatase promoter required for cyclic adenosine 3',5'-monophosphate induction in ovarian granulosa cells and constitutive expression in R2C Leydig cells. *Molecular Endocrinology* 7, 341-354.
- Galarneau, L., Pare, J. F., Allard, D., Hamel, D., Levesque, L., Tugwood, J. D., Green, S., and Belanger, L. (1996). The alpha1-fetoprotein locus is activated by a nuclear receptor of the *Drosophila* FTZ-F1 family. *Mol Cell Biol* 16, 3853-3865.
- Gampe, R. T., Jr., Montana, V. G., Lambert, M. H., Miller, A. B., Bledsoe, R. K., Milburn, M. V., Kliewer, S. A., Willson, T. M., and Xu, H. E. (2000). Asymmetry in the

- PPAR γ /RXR α crystal structure reveals the molecular basis of heterodimerization among nuclear receptors. *Mol Cell* 5, 545-555.
- Giguere, V. (1999). Orphan nuclear receptors: from gene to function. *Endocr Rev* 20, 689-725.
- Glass, C. K., and Rosenfeld, M. G. (2000). The coregulator exchange in transcriptional functions of nuclear receptors. *Genes Dev* 14, 121-141.
- Goodwin, B., Jones, S. A., Price, R. R., Watson, M. A., McKee, D. D., Moore, L. B., Galardi, C., Wilson, J. G., Lewis, M. C., Roth, M. E., *et al.* (2000). A regulatory cascade of the nuclear receptors FXR, SHP-1, and LRH-1 represses bile acid biosynthesis. *Mol Cell* 6, 517-526.
- Greschik, H., Wurtz, J. M., Sanglier, S., Bourguet, W., van Dorsselaer, A., Moras, D., and Renaud, J. P. (2002). Structural and functional evidence for ligand-independent transcriptional activation by the estrogen-related receptor 3. *Mol Cell* 9, 303-313.
- Hammer, G. D., and Ingraham, H. A. (1999). Steroidogenic factor-1: its role in endocrine organ development and differentiation. *Front Neuroendocrinol* 20, 199-223.
- Hammer, G. D., Krylova, I., Zhang, Y., Darimont, B. D., Simpson, K., Weigel, N. L., and Ingraham, H. A. (1999). Phosphorylation of the nuclear receptor SF-1 modulates cofactor recruitment: integration of hormone signaling in reproduction and stress. *Mol Cell* 3, 521-526.
- Hinshelwood, M., Repa, J., Shelton, J., Richardson, J., Mangelsdorf, D., and Mendelson, C. (2003). Expression of SF-1 and LRH-1 in the Mouse Ovary, Localization in Different Cell Types Correlates with Differing Function. *Mol Endocrinol Submitted*.
- Huber, B. R., Desclozeaux, M., West, B. L., Cunha-Lima, S. T., Nguyen, H. T., Baxter, J. D., Ingraham, H. A., and Fletterick, R. J. (2003). Thyroid hormone receptor-beta mutations conferring hormone resistance and reduced corepressor release exhibit decreased stability in the N-terminal ligand-binding domain. *Mol Endocrinol* 17, 107-116.
- Ingraham, H. A., Lala, D. S., Ikeda, Y., Luo, X., Shen, W. H., Nachtigal, M. W., Abbud, R., Nilson, J. H., and Parker, K. L. (1994). The nuclear receptor steroidogenic factor 1 acts at multiple levels of the reproductive axis. *Genes and Development* 8, 2302-2312.
- Ito, M., Yu, R., and Jameson, J. L. (1997). DAX-1 inhibits SF-1-mediated transactivation via a carboxy-terminal domain that is deleted in adrenal hypoplasia congenita. *Molecular and Cellular Biology* 17, 1476-1483.
- Kallen, J. A., Schlaeppli, J. M., Bitsch, F., Geisse, S., Geiser, M., Delhon, I., and Fournier, B. (2002). X-Ray Structure of the hROR α LBD at 1.63 Å. Structural and Functional Data that Cholesterol or a Cholesterol Derivative Is the Natural Ligand of ROR α . *Structure (Camb)* 10, 1697-1707.

- Kerr, T. A., Saeki, S., Schneider, M., Schaefer, K., Berdy, S., Redder, T., Shan, B., Russell, D. W., and Schwarz, M. (2002). Loss of nuclear receptor SHP impairs but does not eliminate negative feedback regulation of bile acid synthesis. *Dev Cell* 2, 713-720.
- Lala, D. S., Syka, P. M., Lazarchik, S. B., Mangelsdorf, D. J., Parker, K. L., and Heyman, R. A. (1997). Activation of the orphan nuclear receptor steroidogenic factor 1 by oxysterols. *Proceedings of the National Academy of Sciences of the United States of America* 94, 4895-4900.
- Lee, Y. K., and Moore, D. D. (2002). Dual mechanisms for repression of the monomeric orphan receptor liver receptor homologous protein-1 by the orphan small heterodimer partner. *J Biol Chem* 277, 2463-2467.
- Liu, D. L., Liu, W. Z., Li, Q. L., Wang, H. M., Qian, D., Treuter, E., and Zhu, C. (2003). Expression and Functional Analysis of Liver Receptor Homologue-1 as a Potential Steroidogenic Factor in Rat Ovary. *Biol Reprod*.
- Lu, T. T., Makishima, M., Repa, J. J., Schoonjans, K., Kerr, T. A., Auwerx, J., and Mangelsdorf, D. J. (2000). Molecular basis for feedback regulation of bile acid synthesis by nuclear receptors. *Mol Cell* 6, 507-515.
- Luo, X., Ikeda, Y., and Parker, K. L. (1994). A cell-specific nuclear receptor is essential for adrenal and gonadal development and sexual differentiation. *Cell* 77, 481-490.
- Luo, Y., Liang, C. P., and Tall, A. R. (2001). The orphan nuclear receptor LRH-1 potentiates the sterol-mediated induction of the human CETP gene by liver X receptor. *J Biol Chem* 276, 24767-24773.
- Maluf, N. K., and Lohman, T. M. (2003). Self-association equilibria of Escherichia coli UvrD helicase studied by analytical ultracentrifugation. *J Mol Biol* 325, 889-912.
- Mellon, S. H., and Bair, S. R. (1998). 25-Hydroxycholesterol is not a ligand for the orphan nuclear receptor steroidogenic factor-1 (SF-1). *Endocrinology* 139, 3026-3029.
- Moraitis, A. N., and Giguere, V. (1999). Transition from monomeric to homodimeric DNA binding by nuclear receptors: identification of RevErbAalpha determinants required for RORalpha homodimer complex formation. *Mol Endocrinol* 13, 431-439.
- Nachtigal, M. W., Hirokawa, Y., Enyeart-VanHouten, D. L., Flanagan, J. N., Hammer, G. D., and Ingraham, H. A. (1998). Wilms' tumor 1 and Dax-1 modulate the orphan nuclear receptor SF-1 in sex-specific gene expression. *Cell* 93, 445-454.
- Nitta, M., Ku, S., Brown, C., Okamoto, A. Y., and Shan, B. (1999). CPF: an orphan nuclear receptor that regulates liver-specific expression of the human cholesterol 7alpha-hydroxylase gene. *Proc Natl Acad Sci U S A* 96, 6660-6665.

- Nolte, R. T., Wisely, G. B., Westin, S., Cobb, J. E., Lambert, M. H., Kurokawa, R., Rosenfeld, M. G., Willson, T. M., Glass, C. K., and Milburn, M. V. (1998). Ligand binding and co-activator assembly of the peroxisome proliferator-activated receptor-gamma. *Nature* 395, 137-143.
- Parker, K. L., Rice, D. A., Lala, D. S., Ikeda, Y., Luo, X., Wong, M., Bakke, M., Zhao, L., Frigeri, C., Hanley, N. A., *et al.* (2002). Steroidogenic factor 1: an essential mediator of endocrine development. *Recent Prog Horm Res* 57, 19-36.
- Pissios, P., Tzamelis, I., Kushner, P., and Moore, D. D. (2000). Dynamic stabilization of nuclear receptor ligand binding domains by hormone or corepressor binding. *Mol Cell* 6, 245-253.
- Ribeiro, R. C., Feng, W., Wagner, R. L., Costa, C. H., Pereira, A. C., Apriletti, J. W., Fletterick, R. J., and Baxter, J. D. (2001). Definition of the surface in the thyroid hormone receptor ligand binding domain for association as homodimers and heterodimers with retinoid X receptor. *J Biol Chem* 276, 14987-14995.
- Roberts, L. M., Shen, J., and Ingraham, H. A. (1999). New solutions to an ancient riddle: defining the differences between Adam and Eve. *Am J Hum Genet* 65, 933-942.
- Sadovsky, Y., Crawford, P. A., Woodson, K. G., Polish, J. A., Clements, M. A., Tourtellotte, L. M., Simburger, K., and Milbrandt, J. (1995). Mice deficient in the orphan receptor steroidogenic factor 1 lack adrenal glands and gonads but express P450 side-chain-cleavage enzyme in the placenta and have normal embryonic serum levels of corticosteroids. *Proc Natl Acad Sci U S A* 92, 10939-10943.
- Schoonjans, K., Annicotte, J. S., Huby, T., Botrugno, O. A., Fayard, E., Ueda, Y., Chapman, J., and Auwerx, J. (2002). Liver receptor homolog 1 controls the expression of the scavenger receptor class B type I. *EMBO Rep* 3, 1181-1187.
- Shiau, A. K., Barstad, D., Loria, P. M., Cheng, L., Kushner, P. J., Agard, D. A., and Greene, G. L. (1998). The structural basis of estrogen receptor/coactivator recognition and the antagonism of this interaction by tamoxifen. *Cell* 95, 927-937.
- Stehlin, C., Wurtz, J. M., Steinmetz, A., Greiner, E., Schule, R., Moras, D., and Renaud, J. P. (2001). X-ray structure of the orphan nuclear receptor RORbeta ligand-binding domain in the active conformation. *Embo J* 20, 5822-5831.
- Steinmetz, A. C., Renaud, J. P., and Moras, D. (2001). Binding of ligands and activation of transcription by nuclear receptors. *Annu Rev Biophys Biomol Struct* 30, 329-359.
- Suzuki, T., Kasahara, M., Yoshioka, H., Morohashi, K., and Umesono, K. (2003). LXXLL-related motifs in Dax-1 have target specificity for the orphan nuclear receptors Ad4BP/SF-1 and LRH-1. *Mol Cell Biol* 23, 238-249.

- Tran, P., Lee, M., Marin, O., Xu, B., Jones, K. R., Reichardt, L. R., Rubenstein, J. L., and Ingraham, H. A. (2003). Requirement of the orphan nuclear receptor SF-1 in terminal differentiation of ventromedial hypothalamic neurons. *Mol Cell Neuroscience In press*.
- Wang, L., Lee, Y. K., Bundman, D., Han, Y., Thevananther, S., Kim, C. S., Chua, S. S., Wei, P., Heyman, R. A., Karin, M., and Moore, D. D. (2002). Redundant pathways for negative feedback regulation of bile acid production. *Dev Cell* 2, 721-731.
- Wang, Z. J., Jeffs, B., Ito, M., Achermann, J. C., Yu, R. N., Hales, D. B., and Jameson, J. L. (2001). Aromatase (Cyp19) expression is up-regulated by targeted disruption of Dax1. *Proc Natl Acad Sci U S A* 98, 7988-7993.
- Watkins, R. E., Wisely, G. B., Moore, L. B., Collins, J. L., Lambert, M. H., Williams, S. P., Willson, T. M., Kliewer, S. A., and Redinbo, M. R. (2001). The human nuclear xenobiotic receptor PXR: structural determinants of directed promiscuity. *Science* 292, 2329-2333.
- Wisely, G. B., Miller, A. B., Davis, R. G., Thornquest, A. D., Jr., Johnson, R., Spitzer, T., Sefler, A., Shearer, B., Moore, J. T., Willson, T. M., and Williams, S. P. (2002). Hepatocyte nuclear factor 4 is a transcription factor that constitutively binds fatty acids. *Structure (Camb)* 10, 1225-1234.
- Xu, H. E., Lambert, M. H., Montana, V. G., Parks, D. J., Blanchard, S. G., Brown, P. J., Sternbach, D. D., Lehmann, J. M., Wisely, G. B., Willson, T. M., *et al.* (1999). Molecular recognition of fatty acids by peroxisome proliferator-activated receptors. *Mol Cell* 3, 397-403.
- Xu, H. E., Stanley, T. B., Montana, V. G., Lambert, M. H., Shearer, B. G., Cobb, J. E., McKee, D. D., Galardi, C. M., Plunket, K. D., Nolte, R. T., *et al.* (2002). Structural basis for antagonist-mediated recruitment of nuclear co-repressors by PPARalpha. *Nature* 415, 813-817.

Acknowledgements

We wish to thank Drs. David Moore, Luc Berenger and Miyuki Suzawa for reagents provided. We also wish to acknowledge Drs. Marion Desclozeaux, Russ Huber, Jennifer Turner, Maia Vinogradova, and Horng Der Ou for initial contributions and advice during this project, and James Holten for help on the beamline 8.3.1. We are especially grateful for the intellectual and technical advice of Giselle Knudsen in the analytical ultracentrifugation analyses. This work was supported by an NIH program project grant (DK 58390) to R.J.F and H.A.I.

Table 1. Data collection and refinement statistics

Crystallization	
Unit cell dimensions	
a (Å)	34.8
b (Å)	127.5
c (Å)	53.2
β (°)	91.7
Space group	P2 ₁
Molecules per asymmetric unit	2
Resolution (Å)	2.4
Number of unique reflections	17954
Data redundancy	6
Completeness ² (%)	98.2 (88.8)
R _{symm} ^{1,2} (%)	6.7 (16.9)
< I/s(I) >	24.4 (5.7)
Refinement (50.0 – 2.4 Å)	
s-cutoff	none
R	21.3
R _{free} ³	23.1
R.m.s. deviation from ideality	
Bond length (Å)	0.009
Bond angle (°)	1.57
Average B-factor (Å ²)	
All atoms	44.8
Protein atoms	44.6
Water molecules	53.6

¹Number in parenthesis is for the last resolution shell (2.5 – 2.4 Å)

²R_{symm} = $\sum_h |I_h - \bar{I}| / \sum_h I$, where (I) is the mean intensity of reflection h

³R_{free} is for 5% of total reflections

Figure 1. Structure of LRH-1 ligand binding domain. (a, b) Ribbon representation of LRH-1 structure shows α -helices and β -strands forming four layers in the sandwiched LRH-1 structure as highlighted with orange, purple, pink and red, respectively. The view on panel b is rotated ~ 90 degree relative to that shown in panel (a). The LRH-1 specific helix H2 (red) forms the fourth and outmost layer in the structure. (c) Superposition of LRH-1 with the RXR LBD bound to ligand (pdb entry 1FBY) depicts LRH-1 in orange, and RXRa with 9-*cis*-retinoic acid in blue.

Figure 2. Architecture of LRH-1 ligand-binding pocket. (a) A fragment of electron density map corresponding to the ligand binding pocket of LRH-1 is shown. A simulated annealing composite omit map based on coefficients $2F_o - F_c$ was calculated for the refined model and is displayed at 1.0 \AA in yellow. Residues forming the walls of the ligand binding pocket with corresponding electron density are shown. The small islands in the vicinity of charged residues, as observed in the electron density maps are most likely water molecules. (b) An approximate position and size of a hypothetical ligand inside the LRH-1 pocket shows 9-*cis*-retinoic acid (in red) from the liganded structure of RXRa LBD superposed with that of LRH-1. (c) Residues forming the LRH-1 ligand binding pocket. Hydrophobic and polar residues depicted as gray and yellow, and positively and negatively charged residues illustrated in red and blue, respectively. The shape of the enveloped cavity of the pocket is indicated by green surface. (d) Mutations inside the LRH-1 ligand binding pocket and their effect on the shape and size of the pocket are shown for one mutant (A368W). (e) The activity of each mutant as indicated on the Y-axis, was tested in HepG2 cells either alone (-) or with increasing amounts of the repressor, SHP, as

indicated on the X-axis. Activity is shown as relative luciferase activity using the AroLuc reporter construct containing the proximal promoter of the rat *cyp19* (aromatase) gene.

Figure 3. Architecture of LRH-1 coactivator cleft. (a) The LRH-1 interface for coactivator binding (orange) is superposed with the corresponding region of active RXR (pdb id 1MZN, light blue) complexed with GRIP1 NR box 2 peptide (royal blue). Structural elements forming the interface are indicated. (b) All family-specific amino acid substitutions at the coactivator binding interface of LRH-1 are highlighted in the atom type-coded colors. Their counterparts in RXR structure are shown in blue. (c) Luciferase activity was measured after increasing amounts of (12, 30, 80, 200 ng per well) pcDNA3-hAIB1, pSG5-GRIP1, RSV-mCBP, pSG5-SMRT, pSG5-SRC1a were added to either wild type pCimLRH1 (40 ng, black bars) or the double cleft mutant (Q398R and N549T, gray bars) in HepG2 cells using the AroLuc reporter (200 ng per well).

Figure 4. Helix 2 provides interface for cofactors recruitment. (a) Ribbon representation of a fragment of structure formed by helices 1, 2, 3 and 9 of LRH1 (orange) or RXR (blue, pdb entry 1FBY) and the positions of the three mutated glutamine residues within H2 of LRH-1 are indicated (Q336A, Q346A, Q347H). (b, c) The activity of wild type pCI mLRH1 (black bars) or mQ3 mutant (gray bars, 40 ng) were assessed in HepG2 hepatoma cells, with or without hAIB1 or mSHP1 by measuring Aroluc reporter activity (200 ng per well). (d) Luciferase activity of pGal-RE-TK (Gal4 reporter) is shown for a mammalian two-hybrid assay employing wild type Gal4-LRH1 DBD (minus DNA binding domain, black bars), or the mQ3 mutant (gray bars) after addition of increasing amounts of VP16 mSHP1.

Figure 5. Structural determinants of LRH-1 oligomerization state. (a) The sedimentation equilibrium profiles for LRH-1 at different concentration (8, 4, and 2 μ M) are shown with absorbance detected at 277 nm as a function of radial position, collected after equilibration for nineteen hours at 8,500 rpm (\blacktriangle), 12,000 rpm (\bullet), and 17,000 rpm (\blacksquare) shown in the upper panel. Data were fitted to single-species model, and the resulting apparent molecular weight is 28.4 kDa (\pm 1.8) corresponds to the calculated weight of the LRH-1 monomer. (b) Hypothetical LRH-1 homodimerization interface is modeled for two LRH-1 ligand binding domains (in orange and red, respectively) based on RXR active homodimers (pdb id 1MZN). Repulsive interactions created by amino acid substitutions (G/E, highlighted in panel c) are indicated. (c) Primary sequence alignment reveals family-specific amino acid substitutions in structural elements participating in the nuclear receptor ligand binding domain dimerization. Critical amino acids are highlighted.

Figure 6. Structural model for LRH-1 activation. (a) Seven structural elements that define the active conformation of ligand-bound RXR are highlighted in blue (ribbons), with the 9 cis-retinoic acid shown in red (stick model)(pdb id 1FBY). (b) Structural elements of the ligand binding pocket contacted directly or indirectly by helix 2 in the LRH-1 LBD are shown in orange, with helix 2 highlighted in red. Packing interactions of the receptor-specific helix H1 preceding H2 are highlighted in pink for both RXR (a) and LRH-1 (b) Residues at the interface between helix H2 and H3 are indicated, and those that are conserved between LRH-1 and SF-1 are underlined. The LRH-1 homologue of the human SF-1 mutant R255L is circled. (d) Superposition of the structural elements of ERR3 (blue, pdb id 1KV6) with corresponding helices H2 and H3 in LRH-1 (orange ribbons) are shown.

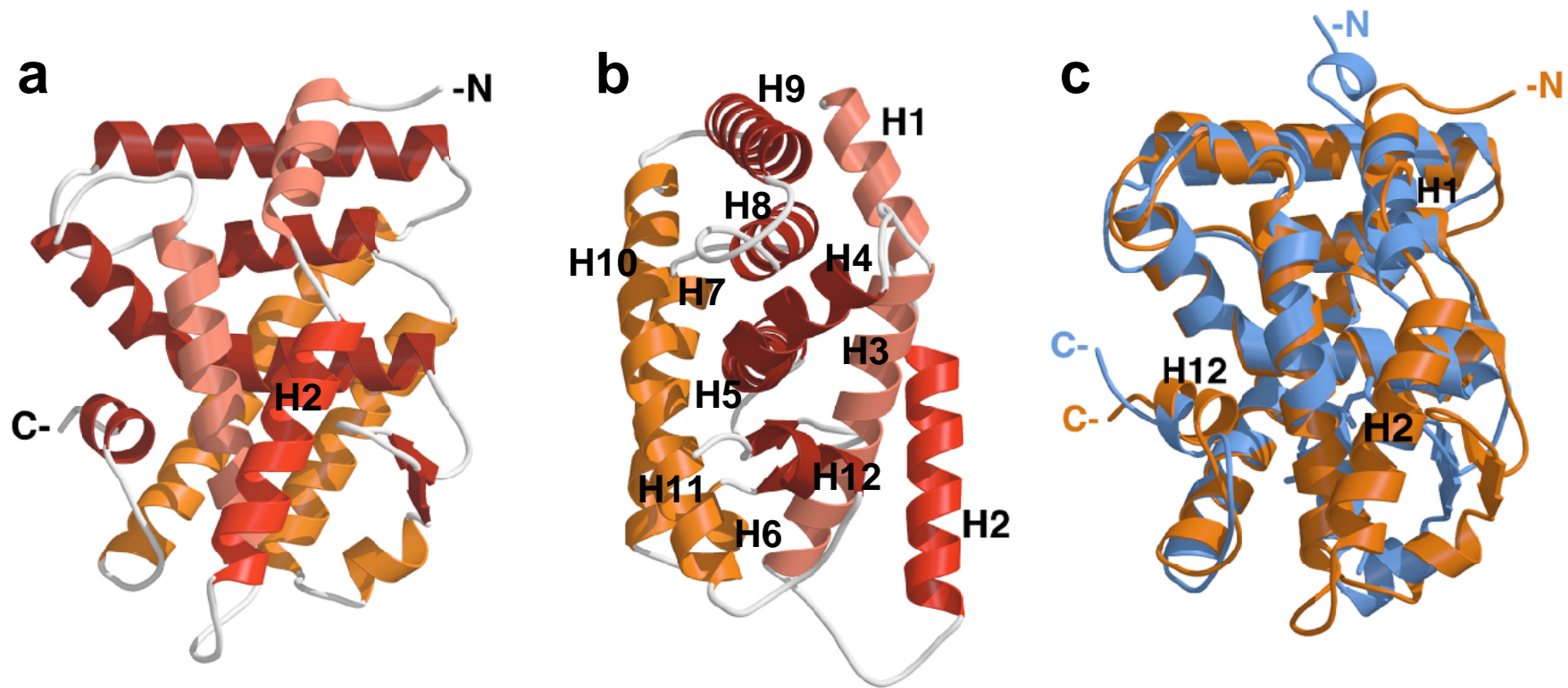


Figure 1 - Sablin/Krylova et al.

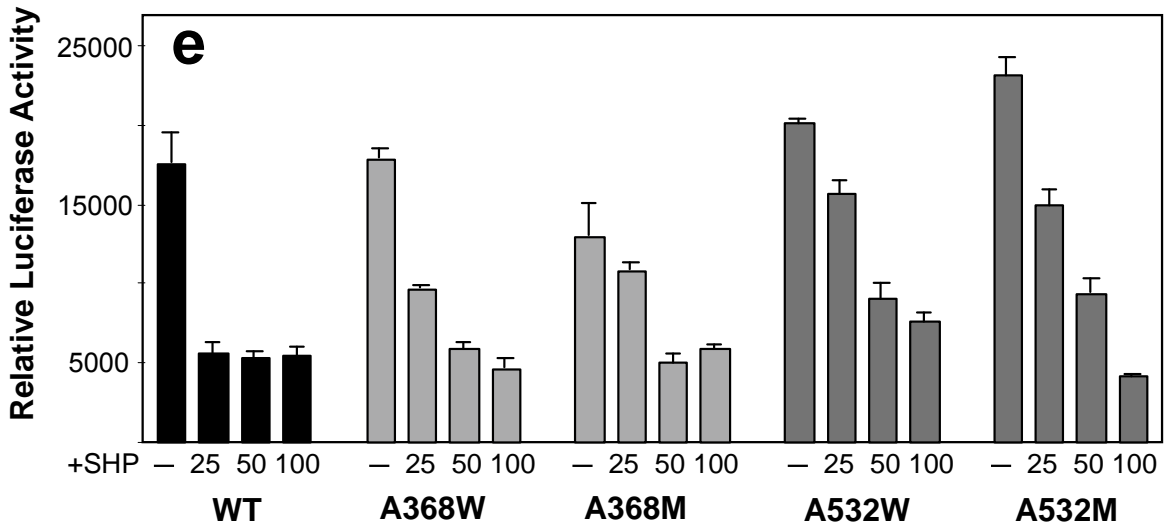
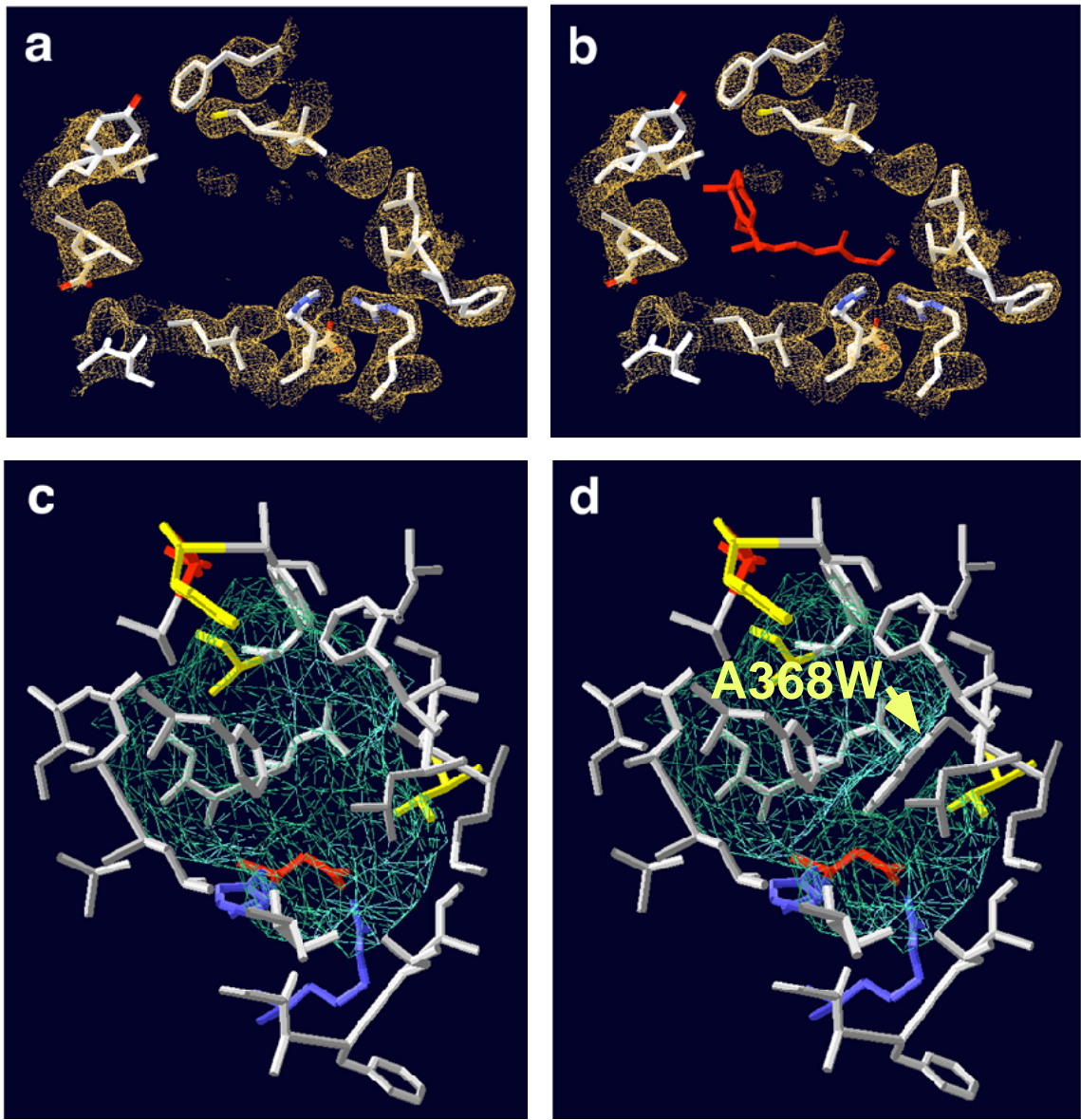


Figure 2 - Sablin/Krylova et al.

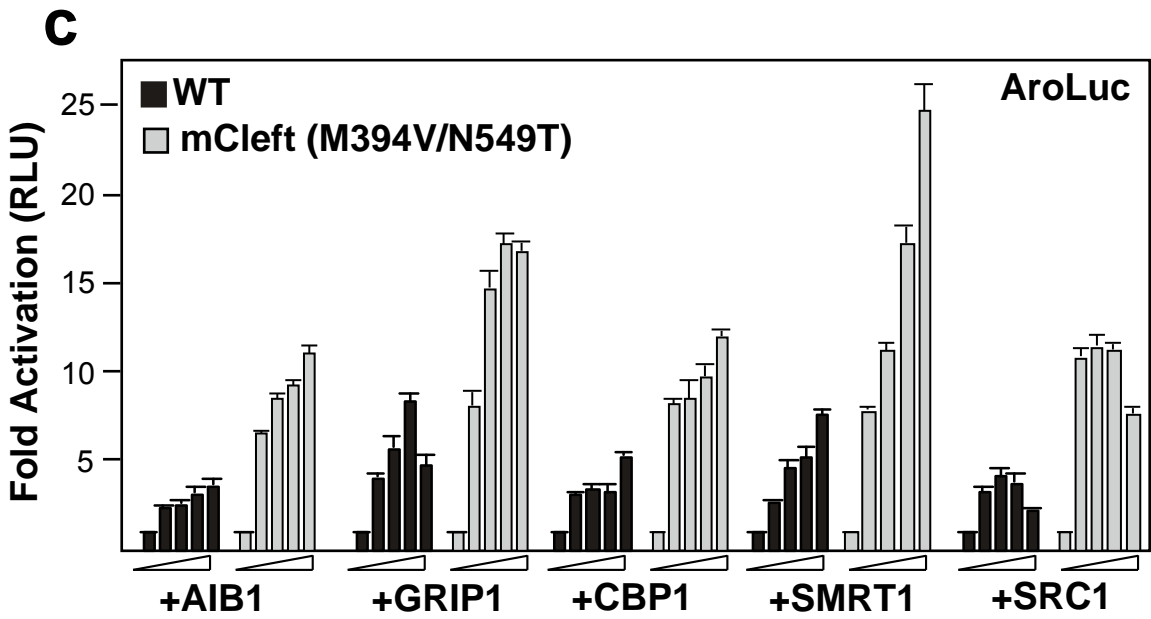
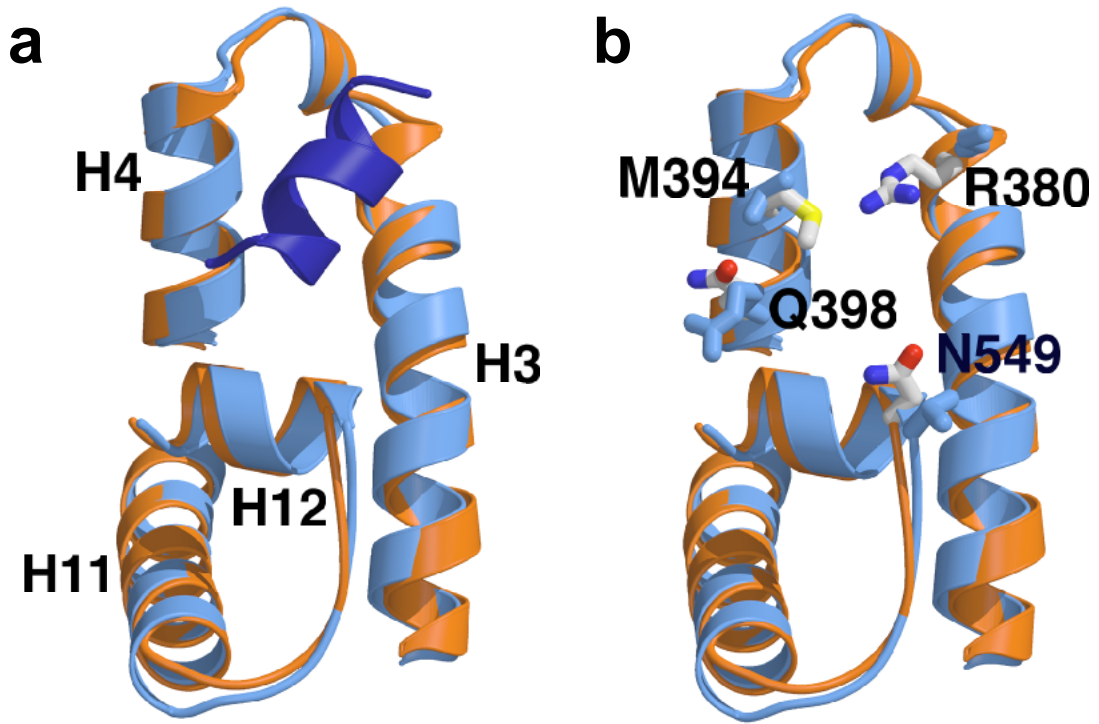


Figure 3 -Sablin/Krylova et al.

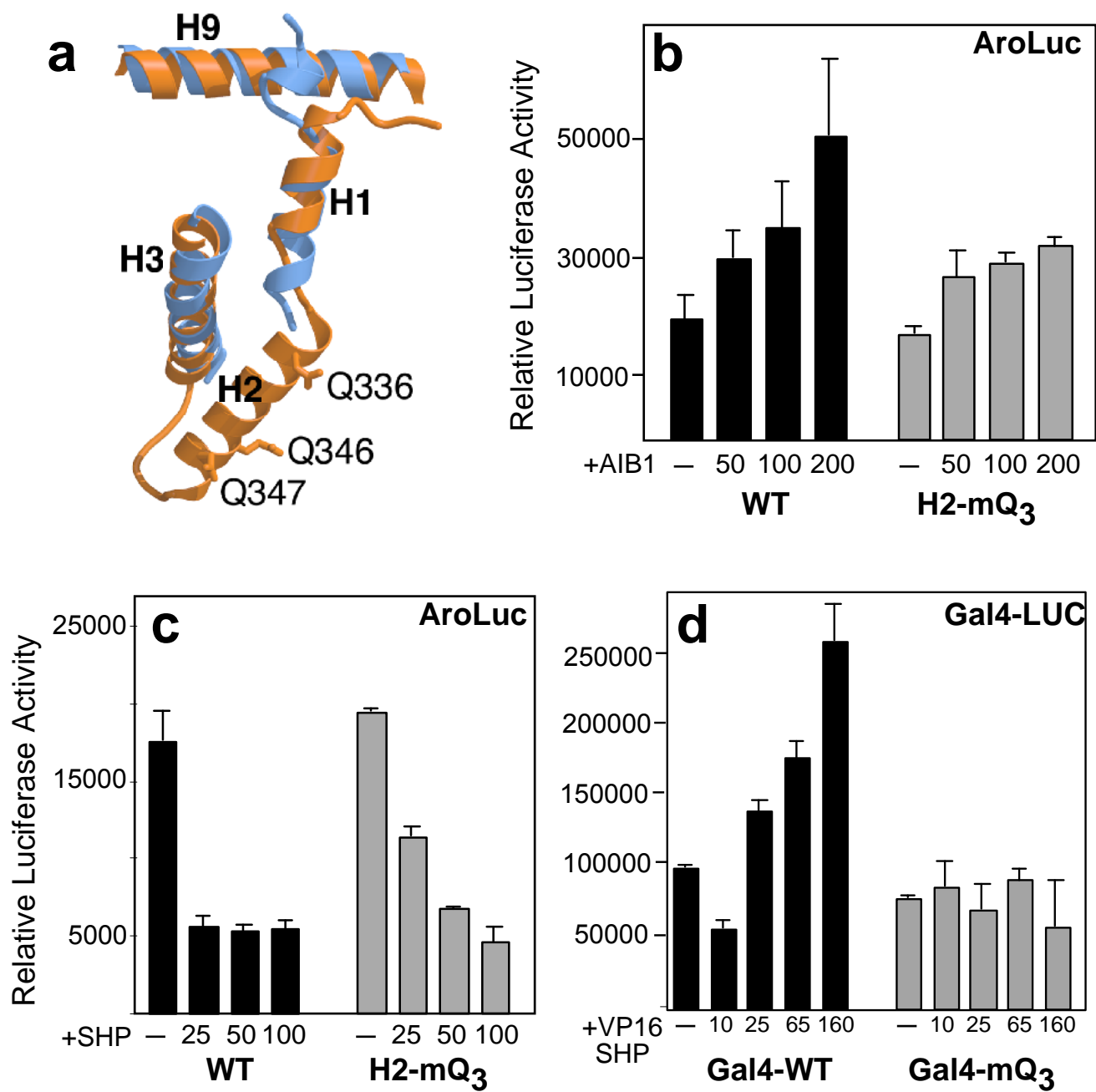


Figure 4 - Sablin/Krylova et al.

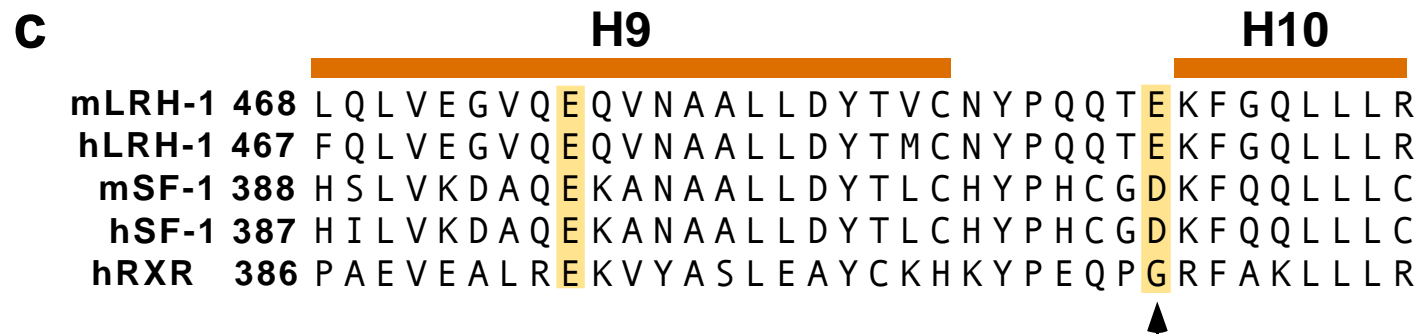
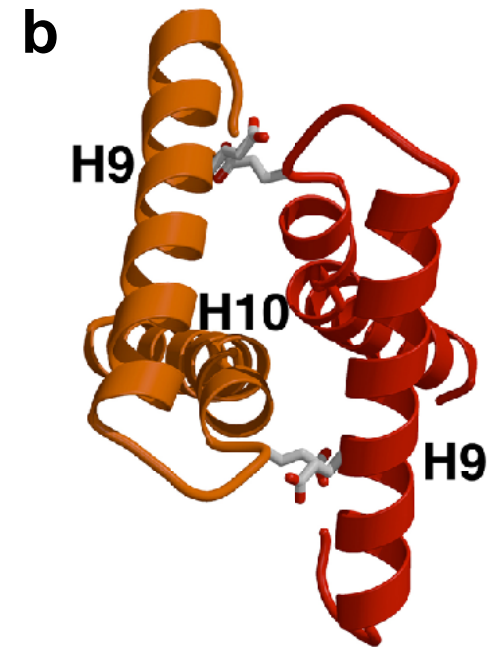
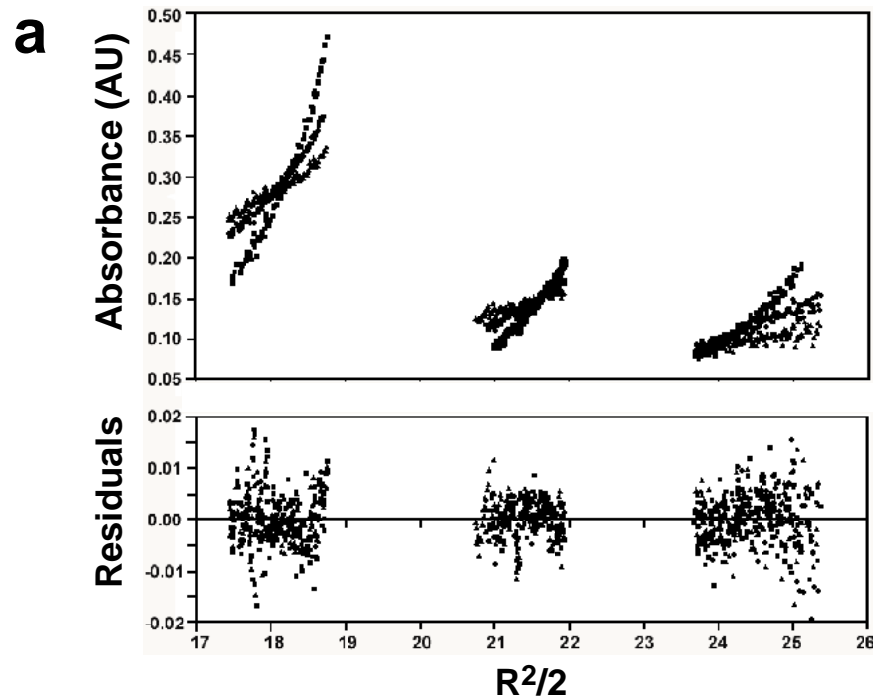


Figure 5 - Sablin/Krylova et al.

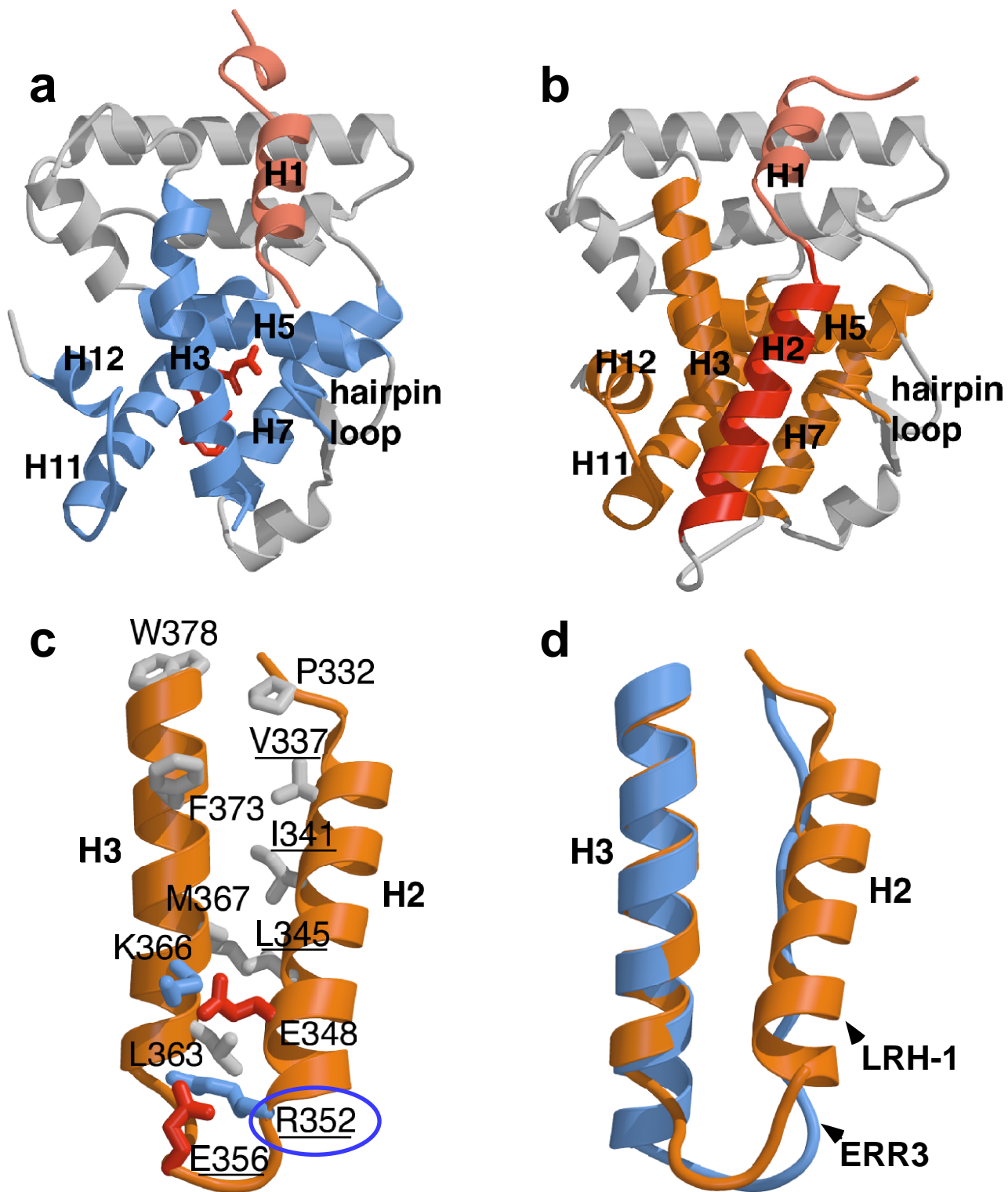


Figure 6 - Sablin/Krylova et al.